

Gabor Wavelets and Gaussian Models to Separate Ground and Non-ground for Airborne Scanned LIDAR Data

Hong Wei and Marc Bartels
School of Systems Engineering
The University of Reading
Reading RG6 6AY, UK

Tel: 44 118 3788608; Fax: 44 118 9751994

h.wei@reading.ac.uk, m.bartels@reading.ac.uk

Abstract

To separate non-ground and ground is the first step of terrain feature classification for remotely sensed LIDAR (Light Detection And Ranging) data. The LIDAR data, which were captured by airborne laser scanner, contain terrain surface height information. This paper aims to segment non-ground (buildings and high vegetation) from ground (flat field) in hilly urban areas. Gabor wavelets were applied to LIDAR data tiles to generate Gabor wavelet features. Training sets of ground and non-ground areas were manually selected from windowed features to establish Gaussian models for the two types of region. In the testing, each window in the Gabor feature space was tested by the probability density function (PDF) of the two models. Maximum likelihood was used in the final classification. The test results have shown that ground areas (flat field) can successfully be segmented from LIDAR data. Most buildings and high vegetation can be detected. In addition, Gabor wavelet transform can remove hill or slope effects on the regular grid LIDAR data by tuning Gabor parameters.

1. Introduction

With advantages of high resolution and accuracy in both horizontal and vertical directions, airborne laser scanned LIDAR data have become popular in remote sensing, land surveying, and land mapping for the last decade [1]. The reflected laser pulses form the Earth surface model, named Digital Surface Model (DSM). An original LIDAR point cloud is registered with the Global Positioning System (GPS) to provide detailed surface information, *e.g.* buildings, vegetation, rivers, flat field, river, basins, etc. Sometimes, the point cloud needs to be interpolated into a regular grid (as a matrix) for post-

process. The development of LIDAR sensors has achieved the high resolution of 0.25m in horizontal, and accuracy of 5-20cm in vertical directions [2]. Compared to the LIDAR sensor technology, LIDAR post-processing becomes as a bottle-neck to put the technology in real uses [3]. This placed a demand for development of algorithms which can automatically interpret LIDAR data. In some applications, *e.g.* flood modelling, the bare-Earth model, called Digital Terrain Model (DTM) is required [4]. From the DSM to DTM, the very first step is to remove buildings and high vegetation from the LIDAR data (point cloud or regular grid). Maas suggested to apply a filter bank to regular grid data for reducing effect of hilly terrain [5] in generation of building model. Existing techniques, *e.g.* wavelet decomposition, did not take orientation into account for the purpose of DTM generation from DSM. Our work in this paper aims to segment buildings and high vegetation (trees and bushes) from the ground (flat fields) in hilly urban areas. The methodology that we proposed is to use regular grid 2D LIDAR data and treat the height information as intensity in order to exploit texture analysis techniques established in image processing.

Gabor filters have been widely used in image texture analysis due to their nature of spatial locality, orientation selectivity, and frequency characteristic [6, 7]. Gabor wavelets model the receptive field profiles of cortical simple cells [8], and they are optimally localised in the space and frequency domain [9]. Gabor wavelet representation captures salient visual properties, *e.g.* discontinuity in gradient. It is popular in the pattern recognition and image processing communities for texture segmentation. Dunn, *et. al.* declared that distinct discontinuities occur only if the Gabor filter parameters are suitably chosen [10]. They then devised a rigorously based method for designing Gabor filters in texture segmentation. Kyrki, *et. al.* worked in a simple Gabor

feature space for invariant object recognition [11]. Randen, *et. al.* suggested in [12] that the Gabor filter bank might be good in texture segmentation for different types of texture images based on scale, orientation, and frequency tuning.

In this paper, Gabor wavelets are applied to airborne laser scanned LIDAR data to generate Gabor wavelet features. Gaussian models are used to classify ground and non-ground based on these features. The paper is organised as follows. Section 2 presents the integrated algorithms used in the segmentation, which includes Gabor wavelet transformation and Gaussian model establishment. The testing results are demonstrated in Section 3 with relevant discussions. Section 4 concludes the work and points out limits for further investigation.

2. Methodology integration

Figure 1 illustrates the combination scheme used in the segmentation. LIDAR tiles as 2D texture maps were imported first. Gabor wavelets were applied to these maps to create a Gabor feature space, which is then grouped into small windows as segmentation units. Training sets of ground and non-ground were manually selected from these windows to establish Gaussian models for the two types of regions. In the testing, each window was checked by the probability density functions of the two Gaussian models, *ie.* pdf_g for ground and pdf_{ng} for non-ground. The Maximum Likelihood was used to classify ground and non-ground as indicated in Figure 1.

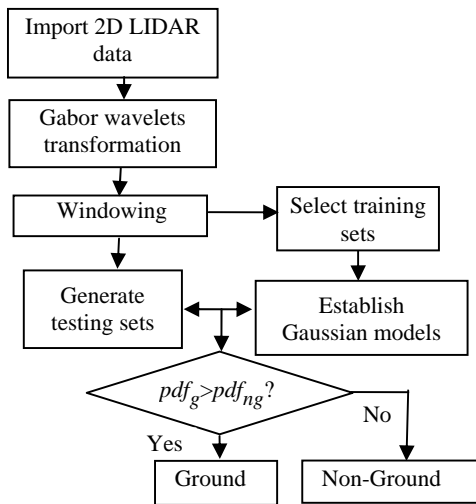


Figure 1. The scheme of segmentation algorithms

2.1 Gabor wavelet representation

In the spatial domain, 2D Gabor wavelets can be expressed by a Gaussian kernel modulated by a complex plane wave [7].

$$g_{\mu,\nu}(x, y) = \frac{\|k_{\mu,\nu}\|^2}{2\pi\sigma^2} e^{-\frac{\|k_{\mu,\nu}\|^2(x^2+y^2)}{2\sigma^2}} [e^{ik_{\mu,\nu}(x+y)} - e^{-\frac{\sigma^2}{2}}] \quad (1)$$

where $k_{\mu,\nu}$ is the wave vector defined by both orientation μ and scale ν , and is constructed as

$$k_{\mu,\nu} = k_\nu e^{i\phi_\mu} \quad (2)$$

In Equation (1), the first term in the square bracket is the oscillatory part in the Gabor kernel, and the second term contributes to the property of DC free. The parameter σ determines the ratio of the Gaussian window width and wavelength. In Equation (2),

$$k_\nu = \frac{k_{\max}}{f^\nu} \quad \text{and} \quad \phi_\mu = \frac{\pi\nu}{4}$$

$k_{\max} = \frac{\pi}{2}$ to ensure sufficient wavelets in the kernel, and

$f = \sqrt{2}$, which is the spacing factor between kernels in the frequency domain. Three scales and four orientations of Gabor wavelets were tested as $\nu \in \{0, 1, 2\}$ and $\mu \in \{0, 1, 2, 3\}$. Figure 2 shows the real part of these Gabor kernels and their magnitude, with $\sigma = 2\pi$.

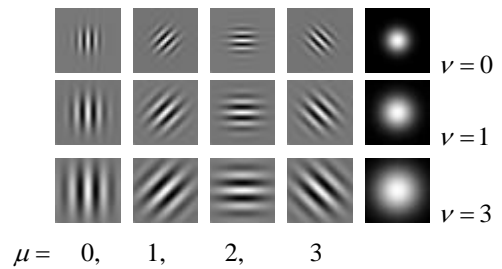


Figure 2. Gabor wavelets

Gabor wavelet representation of 2D LIDAR data $d(x, y)$ is defined as

$$r_{\mu,\nu}(x, y) = d(x, y) * g_{\mu,\nu}(x, y) \quad (3)$$

where $*$ denotes the convolution operator in the spatial domain, and $r_{\mu,\nu}(x, y)$ is the Gabor wavelet representation corresponding to the kernel at

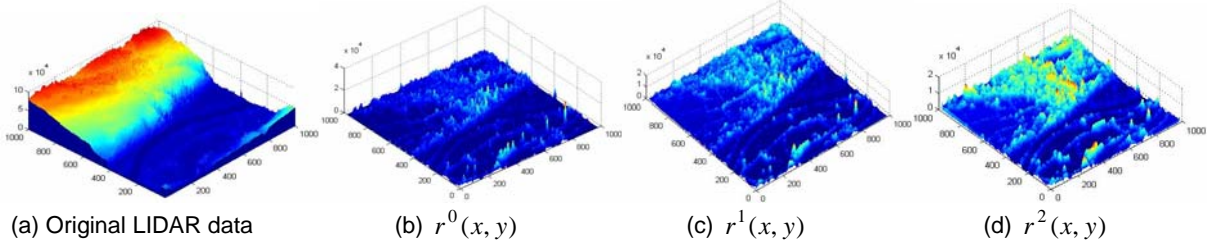


Figure 3. LIDAR data (Copyright © Environment Agency) and its Gabor wavelet representation in three scales

orientation μ and scale ν . It has its complex structure with real part $\Re\{r_{\mu,\nu}(x, y)\}$ and imaginary part $\Im\{r_{\mu,\nu}(x, y)\}$. We use its magnitude as the response, which can be written as

$$\|r_{\mu,\nu}(x, y)\| = \sqrt{\Re^2\{r_{\mu,\nu}(x, y)\} + \Im^2\{r_{\mu,\nu}(x, y)\}} \quad (4)$$

Gabor features reflect local discontinuities with orientation selectivity. Taking this into account, we mixed all Gabor features in the same scale to generate the mixture of the representation as

$$r^\nu(x, y) = \sum_{\mu=0}^3 \omega_\mu \|r_{\mu,\nu}(x, y)\| \quad (5)$$

where ω_μ is a weight assigned to each orientation responses, and satisfies $\sum_{\mu=0}^3 \omega_\mu = 1$. In experiments,

various combinations were tested regarding weight allocation to make sure no directional information loss.

Figure 3 demonstrates a mesh of a LIDAR tile and its Gabor wavelet representations in the three scales. The observation from the experimental analysis indicates that the Gabor wavelet representation with $\nu=0$ removes the slope entirely, while the others can only partially remove the slope in the data. It is important to tune the parameters in Gabor wavelets for the purpose of slope removal in real applications.

2.2 Establishment of Gaussian models

Gaussian models are used for representing ground and non-ground classes in segmentation. We sub-divide the Gabor wavelet representation into small windows with size of $m \times n$. Training sets for the two classes are manually selected from these windows. The selection of window size was tested for the purpose of optimisation in experiments. The probability density function (*pdf*) for ground and non ground classes can be established as

$$pdf_g(\bar{w}_i | \omega_g) = \frac{1}{\sqrt{2\pi}\sigma_g} e^{-\frac{(\bar{w}_i - \bar{\mu}_g)^2}{2\sigma_g^2}} \quad (6)$$

$$pdf_{ng}(\bar{w}_i | \omega_{ng}) = \frac{1}{\sqrt{2\pi}\sigma_{ng}} e^{-\frac{(\bar{w}_i - \bar{\mu}_{ng})^2}{2\sigma_{ng}^2}} \quad (7)$$

where ω_g and ω_{ng} are two classes defined as ground and non-ground; $\bar{\mu}_g, \sigma_g, \bar{\mu}_{ng},$ and σ_{ng} are parameters from windows of the training sets, and represent mean and standard deviation of ground and non-ground, respectively. The variable \bar{w}_i is the mean of each window in the Gabor wavelet space, written as

$$\bar{w}_i = \frac{1}{m \times n} \sum_{ii=1}^m \sum_{jj=1}^n r^\nu(x_{ii}, y_{jj}),$$

where $i \in \{1, 2, \dots, N\}$ represents the number of windows used in segmentation.

During the classification, each window was tested, and its values of pdf_g and pdf_{ng} were compared. If $pdf_g > pdf_{ng}$, the window is assigned as ground; otherwise it is non-ground as depicted in Figure 1.

3. Test results and discussions

LIDAR data we used in the test were supplied by the UK Environment Agency (EA). LIDAR data tiles were processed by using the developed algorithm. The validation was carried out by using related optical data which were also provided by the EA. Figure 4 demonstrates the optical data and the segmentation results of three tiles. Figures 4 (b), (d) and (f) clearly demonstrate that flat fields were accurately segmented without effects of slope in the original LIDAR data. The segmentation results were generated by using Gabor wavelet representation in the scale of $\nu=0$. The reason was that it provided better solutions for slope removal. In the experimental analysis, it was also observed that the kernel frequency controlled by the value of σ affected the responses of Gabor wavelets. For Tile 2, the

Gabor wavelets were generated by tuning $\sigma = \pi$. Rivers were segmented by using absolute height information from LIDAR data.

Investigation brought a problem up to the surface, *i.e.* large flat roof buildings may also be classified as a flat field (see Figure 4(d) and 4(e) as circled). This is because there is continuous gradient in the area of the roofs. This requires other methods to be employed for further processing. The elevation information from the original data can be used for local height estimation. We leave this problem for the future research.

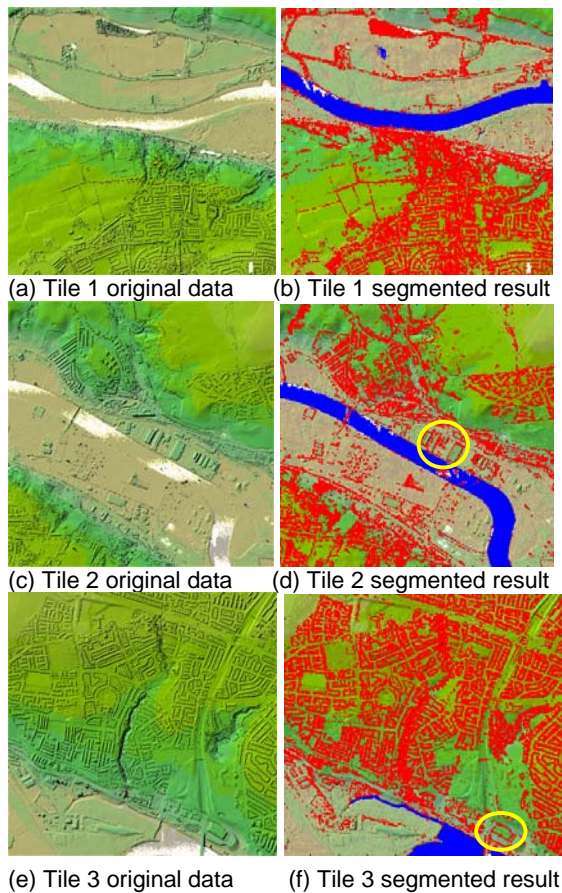


Figure 4. Test results

4. Conclusions

We developed an algorithm aiming to segment non-ground (*e.g.* buildings and high vegetation) from ground (flat fields) in airborne scanned LIDAR data. This is the very first step for terrain feature classification based on LIDAR data. The developed algorithm segments flat fields accurately with very low false negative. It is important in real applications to exclude this type of data to reduce computation expenses. The false positive

problem as the flat roof of large buildings has to be faced. We use those data segmented as non-ground in the further study of terrain feature classification. In that stage, other techniques, such as data fusion will be introduced, and more classes will also be defined.

5. Acknowledgement

We would like to thank the UK Environment Agency for supplying LIDAR data. The project is partially funded by RETF of the University of Reading.

6. References

- [1] H. G. Maas, Akquisition von 3D-GIS Daten durch Flugzeuglaserscanning, *Kartographische Nachrichten*, 55(1), 2005, pp. 3-11
- [2] E. J. Huising and L. M. Gomes Pereira, "Errors and Accuracy Estimates of Laser Data Acquired by Various Laser Scanning Systems for Topographic Applications", *ISPRS Journal of Photogrammetry & Remote Sensing*, vol. 53, 1998, pp. 245-261
- [3] T. T. Vu, M. Matsuoka, and F. Yanmazak, "LIDAR Signatures to Update Japanese Building Inventory Database", *Asian Conference of Remote Sensing*, Chianmai, Thailand, November 2004, pp. 624-629
- [4] S. J. Maybank, R. V. Fraile, V. Prinnet, F. Wang, Z. H. Zhang, and G. Wu, "Scene Modeling from Remote Sensing Data", *Workshop on Information Technologies for Flood Management*, Beijing, 17 Sept. 2001
- [5] H.-G. Maas and G. Vosselman, "Two Algorithms for Extracting Building Models from Raw Laser Altimetry Data", *ISPRS Journal of Photogrammetry & Remote Sensing*, Vol. 54, 1999, pp. 153-163
- [6] Anil K. Jain and Farshid Farrokhnia, "Unsupervised Texture Segmentation Using Gabor Filters", *Pattern Recognition*, vol. 24, no. 12, 1991, pp. 1167-1185
- [7] Chengjun Liu, "Gabor-based Kernel PCA with Fractional Power Polynomial Models for Face Recognition", *IEEE Transaction on Pattern Analysis and Machine Intelligence*, vol.26, no.5, 2004, pp. 572-581
- [8] J. G. Daugman, "Two-Dimension Spectral Analysis of Cortical Receptive Field Profiles", *Vision Research*, vol. 20, 1980, pp. 847-856
- [9] Tai Sing Lee, "Image Representation Using 2D Gabor Wavelets", *IEEE Transaction on Pattern Analysis and Machine Intelligence*, vol.18, no.10, 1996, pp. 959-971
- [10] D. Dunn and W. E. Higgins, "Optimal Gabor filters for Texture Segmentation", *IEEE Transaction on Image Processing*, vol. 4, no. 7, 1995, pp. 947-964
- [11] V. Kyrki, J. K. Kamarainen, and H. Kalviainen, "Simple Gabor Feature Space for Invariant Object Recognition", *Pattern Recognition Letters*, vol.25, no. 3, 2004, pp. 311-318
- [12] T. Randen and J. H. Husoy, "Filtering for Texture Classification: A Comparative Study", *IEEE Transaction on Pattern Analysis and Machine Intelligence*, vol. 21, no. 4, 1999, pp. 291-31